X-622-68-26
PREPRINT

NASA TM X-63112

A VERY HIGH RESOLUTION RADIOMETRIC EXPERIMENT FOR ATS F AND G

I. L. GOLDBERG

JANUARY 1968

GSFC
GODDARD SPACE FLIGHT CENTER
GREENBELT, MARYLAND

X-622-68-26

A VERY HIGH RESOLUTION RADIOMETRIC EXPERIMENT FOR ATS F AND G

I. L. Goldberg

January 1968

Goddard Space Flight Center
Greenbelt, Maryland

CONTENTS

A VERY HIGH RESOLUTION RADIOMETRIC EXPERIMENT FOR ATS F AND G

by

I. L. Goldberg

ABSTRACT

The synchronous altitude satellite offers a unique opportunity to continuously observe cloud cover and cloud motion over a large portion of the earth. It is proposed to use a scanning radiometer operating in the 10.5 to 12.5 micron spectral region to make these observations and surface temperature measurements both night and day. A radiometer containing an 8-inch aperture diameter Cassegrain telescope and a cooled (77°K) detector can make accurate temperature measurements with an effective subsatellite ground resolution of approximately 8 nautical miles. The analysis shows that because of diffraction effects and sensitivity requirements this resolution is about the best that can be attained with the 8-inch aperture radiometer. Over half of the estimated system weight of 110 pounds is due to the solid cryogen cooler. Because of the poor location space available on the spacecraft it does not appear feasible to use the much lighter radiative cooler.

A VERY HIGH RESOLUTION RADIOMETRIC EXPERIMENT FOR ATS F AND G

I. EXPERIMENTAL OBJECTIVES

The primary purpose of this experiment is to continuously observe cloud cover and cloud motion over a large portion of the earth's surface with a scanning radiometer operating in the 10.5 to 12.5 micron region. The proposed resolution is approximately 1,000 lines per frame and an I.F.O.V. (instantaneous field of view) of 0.3 mrad (the effective I.F.O.V. will be somewhat larger because of diffraction effects). Because of size and weight limitations it is not feasible to achieve the spatial resolution of the ATS spin-scan camera experiment (2,000 lines and a 0.1 mrad I.F.O.V.). On the other hand, the infrared radiometer has several important advantages over a camera that senses visible radiation. First, the familiar "full earth" pictures made with the ATS camera can be taken only during a small fraction of the day, while other pictures taken during the 24 hour period show varying smaller portions of the earth, depending on the location of the terminator. However, the radiometer system will take "full earth" pictures on every frame, independent of the position of the terminator. In fact, the terminator may not even be detected. Second, the radiometer has the added capability of temperature measurement (cloud top altitude can be inferred from cloud top temperature and sea surface temperature variations such as those due to the Gulf stream can be observed in cloud free regions).

The importance of this type of experiment was recognized in the report of the Global Atmospheric Research Programme (GARP) Study Conference written by the ICSU/IUGG Committee on Atmospheric Sciences (the conference was held in Stockholm, Sweden from June 28-July 11, 1967 and was sponsored by IUGG, COSPAR and the World Meteorological Organization).

The ATS offers several advantages over near earth satellites. Continuous coverage over the same large area makes it possible to infer wind speeds at cloud top altitudes. It also permits observations of the birth of hurricanes (or typhoons). In addition, all the data are continuously transmitted to the ground station. Near earth satellites, at the present time, must carry tape recorders to store all the information collected throughout the orbit. Elimination of the need for data storage on the spacecraft is not a trivial benefit.

II. RADIOMETER DESCRIPTION

An optical schematic of the radiometer is shown in Fig. 1. Radiation from the scene is reflected from the scan mirror into a Cassegrain telescope and is brought to a focus at the chopper. An optical relay is used to increase the speed of the system and focus the modulated radiation onto the cooled detector. Because the ATS F&G satellites will be at synchronous altitude and three-axis stabilized, scanning in both latitude and longitude directions, must be accomplished by the radiometer optical system. This can be done with a nodding scan mirror (moved by two drives at right angles to each other).

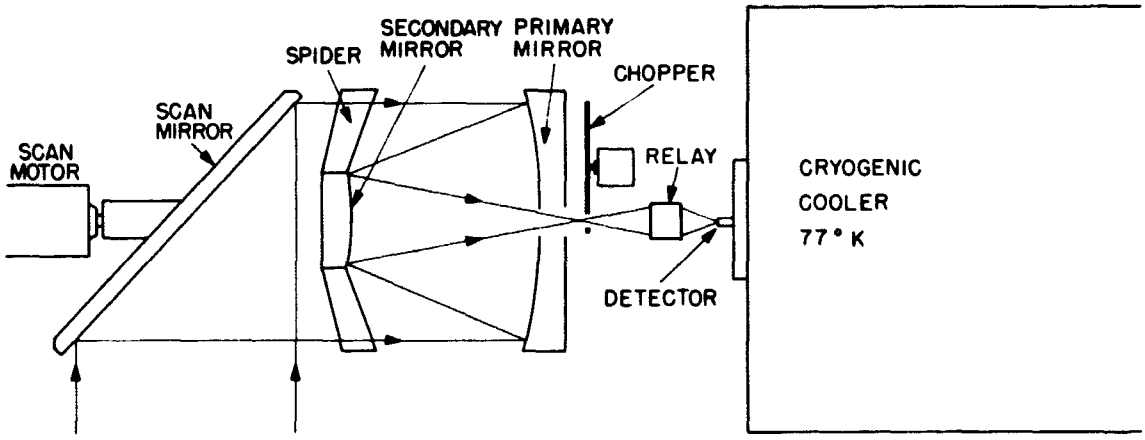

Figure 1–Optical Schematic of Radiometer

Because of the very high angular resolution (0.3 mrad instantaneous F.O.V.) it is necessary to employ an optical system close to the diffraction limit in order to keep the optics to a reasonable size. An 8-inch diameter telescope appears to be feasible from both the standpoint of diffraction and signal-to-noise ratio. The effect of diffraction in degrading the spatial resolution will be discussed later.

Aperture imaging is not recommended for this system even though it produces a uniformly irradiated image (from an unobstructed aperture). The primary disadvantage of an aperture imaging system is that a shift of the detector with respect to the image (especially in the lateral direction) causes a degradation in signal since a part of the image falls off the detector. Also, for a folded optical system the image of the aperture is not completely uniform due to the secondary mirror and spider (supports for the secondary). When the detector itself acts as the field stop a small lateral shift is equivalent to a small shift in the view

angle, but with no loss of energy. In addition, nonuniformities within the instantaneous field image have a tendency to be smoothed out by the diffraction effects in this system, so that there is essentially no advantage in using an aperture imaging technique. Because of the scan mirror motion a lateral shift of the detector, in the field imaging case, will also cause a rotation of the field angle, which is of little importance because of the small angular amplitude of the scan mirror motion.

Since the difficulty of making large diffraction limited telescopes increases rapidly with the optical speed of the system it is important to use a reasonably slow telescope. However, the speed of the telescope cannot be very slow since this would result in a massive instrument. An f/3 telescope seems to be a good compromise. The optical relay can then make the effective f-number of the system smaller. The relay can be either reflective or refractive. If an additional channel is required, say, using the visible region, a reflective relay should be used, along with a dichroic filter, additional optics, a visible detector, associated electronics and perhaps inflight visible calibration source. At the present time we shall assume that the radiometer contains a single channel and that a relay containing germanium lenses is used. The design speed of the relay depends on two factors, (1) the fastest diffraction limited appropriate size lenses available and (2) the smallest detectors available. For example, an f/1.5 relay* in this optical system requires a detector 0.0036 inch (90 microns) on a side. This is close to the limit for both factors and therefore these numbers will be used in determining signal-to-noise ratios. Although not an essential feature, the optical relay makes the task of optical alignment easier.

It is important that the chopper aperture does not serve as a true field stop. The aperture should be greater than the primary image by a factor large enough to ensure that a lateral displacement of the detector (e.g., upon cooling down to operating temperature) does not cause any energy loss due to obscuration. Also the aperture should be large enough so that the detector sees no part of the diffraction pattern caused by the aperture circumference. The aperture can be covered by a shutter near sunrise and sunset to prevent direct sunlight from falling on the detector.

The direction of scanning deserves some attention. The earth picture can be generated by a set of latitude or longitude scan lines (or at some intermediate angle). If the scan direction is perpendicular to the equatorial plane then in the vicinity of the equatorial horizons the radiometer will view a small fraction of the earth within a scan line. Thus near sunrise and sunset the detector can be shielded from the sun with only a small information loss.

*The f-number of the first lens of the relay is f/3 to match the telescope

At the beginning (or end) of each frame a six-step voltage calibration set should be generated. If feasible, two such calibration sets can be used. One voltage calibration staircase can readily be introduced at the output of the amplifier to check the system between the radiometer output and ground station display. The other set can be inserted at the input to the preamplifier to check the radiometer electronics (this requires more careful design).

A summary of the design parameters of the proposed radiometer is given in Table 1.

Table 1. Radiometer design summary

Spectral region: 10.5–12.5 microns
Telescope: 8-inch diameter f/3 Cassegrain
Optical relay: f/1.5 germanium aspheric (first lens f/3)
Geometric I.F.O.V.: 0.3 mrad × 0.3 mrad
Geometric subsatellite ground resolution: 6 n.mi.
Effective I.F.O.V.: 0.4 mrad × 0.4 mrad
Effective subsatellite ground resolution: 8 n.mi.
Number of lines per picture frame: 1,000
Frame size: 18° × 18°
Frame time: 20 minutes
Detector detectivity: 1.5×10^{10} cm $Hz^{1/2}$ $watt^{-1}$
Detector temperature: 77°K
Detector dimensions: .0036 inch × .0036 inch (90 microns)
Information bandwidth: 450 Hz
NEΔT: < 3°C at 200°K
< 0.8°C at 300°K
NET: 145°K
NER: 0.21 W/M^2/STER
Radiometer size, less cooler: 10-inch diameter, 28 inches long
Cryogenic cooler size: 13-inch diameter, 16 inches long
Total weight: 110 pounds
Power consumption: 20 watts

III. DETECTOR COOLING

At present only two types of refrigerator systems are feasible for this experiment – sublimation and radiative coolers. A brief description of both types is given below.

A. Sublimation Cooler

The Lockheed Aircraft Corporation, under contract with NASA/GSFC, has built an engineering model of a solid cryogenic cooler that can maintain a detector at 50°K. It weighs 35 pounds, not including mounting plates or housing. Laboratory tests indicate that the refrigerator when surrounded by room temperature radiation, has a useful space life of six months. With further improvements (this was the first model) the lifetime can be considerably increased. This system uses solid argon as the primary cryogen, surrounded by solid carbon dioxide. In addition to two fill lines (for the two cryogens) there are two lines for a liquid nitrogen heat exchanger to freeze the argon and carbon dioxide. The refrigerator, which is wrapped with multilayer insulation, has a cylindrical shape, 13 inches in diameter by 15 inches long. For 75°K operation either an argon-carbon dioxide or methane-carbon dioxide system would have a lifetime of one year and weigh between 45 and 65 pounds (including mount and housing).

Before launch the cooler must be either purged (with helium or neon) or evacuated to prevent condensation when it is filled and the cryogens are frozen. If an evacuation technique is employed it is necessary to encase the cooler with an aluminum bottle. If purging is feasible, a fiberglass case is sufficient. The aluminum bottle increases the cooler weight from 45 to 65 pounds. As of now it appears that the evacuation technique must be used.

B. Radiative Cooler

The ITT Industrial Laboratories have developed an 80°K two-stage radiative cooler for NASA/GSFC. This company built the Nimbus HRIR which employed a single stage, single-ended radiative cooler that maintained a detector at about 200°K. The present cooler is double-ended (looks at space out of both ends of a highly reflective cone, 180°apart). There are two black cooling patches suspended inside the cooler. The second stage cone is attached to the first stage cold patch which attains a temperature of 180°K. The second stage patch which is conductively coupled to the detector, is suspended inside the second stage cone. It takes about 24 hours to reach the equilibrium temperature of 80°K. The cooler is bulky (10.5" × 23.5" × 20.7") and weighs 20 pounds. The required view angles for each of the two ends of the cone are 60° × 120°.

ITT has made a preliminary study of a single-ended cooler that is more desirable since it would considerably decrease location problems on a spacecraft (needs clear space on one side only). It would be lighter (15 pounds) and somewhat less bulky (volume of 4,000 cm^3 instead of 5,000 cm^3). The solid angle required for viewing space is 60° × 90°. Size and weight can be reduced at the sacrifice of increased view angle.

While the radiation cooler has the advantage of indefinite lifetime and smaller weight, it's location on a spacecraft is more restrictive than that of the sublimation cooler. Normally, a three-axis stabilized spacecraft at synchronous altitude would be a good place to use a radiative cooler. However, for ATS F&G the only location available for the radiometer appears to be inside the struts near the 30-foot antenna (or midway between the earth viewing module and antenna). Since the spacecraft is steerable it will be pointed in different directions at various times. While these conditions do not absolutely rule out the use of a radiative cooler it poses quite a problem. It is safer and easier to employ a sublimation cooler under these constraints.

IV. ANALYSIS

Fundamentally, a radiometer measures radiant flux within its instantaneous field of view (I.F.O.V.) and spectral interval ($\Delta\lambda$). If the source or target fills the I.F.O.V. and there is no reflected energy within $\Delta\lambda$ the radiometer measures the source radiance within $\Delta\lambda$ providing the intervening path is transparent to the radiation of interest. If the source is uniform and radiates as a blackbody within $\Delta\lambda$ the source temperature can be determined from the radiance measurement. Radiometers are frequently calibrated in terms of temperature directly by using a known blackbody source. The radiometer can then measure unknown targets in terms of equivalent blackbody temperature or radiance temperature. In the 10.5 to 12.5 micron atmospheric window region, clouds, water and land features resemble blackbodies reasonably well. In this wavelength interval reflected solar radiation is negligible compared to terrestrial emission so that even during daytime the measured radiance temperature is close to the true target temperature. If target emissivity and atmospheric transmission are taken into account the actual target temperature can be determined accurately.

A. Temperature Discrimination

One of the most important properties of a scanning radiometer is radiance discrimination or the ability to detect changes in radiance as the scene is scanned. These changes can be caused by variations in temperature, emissivity and atmospheric transmission. In the 10.5 to 12.5 micron region atmospheric transmission varies very gradually along a scan line and has a small effect on the received energy (the effect is pronounced in the vicinity of the horizon, however). For the present, atmospheric attenuation will be ignored. The emissivities of clouds, ocean and land features are high in the proposed spectral region (above 0.9) so that the effect of emissivity variations along a scan line will be relatively small (but not negligible). The primary cause of changing radiance values is therefore due to differences in surface temperature. It is because of this that we

often speak of the temperature discrimination capability of the radiometer. The relationship between total radiance (over all wavelengths) change and temperature change of graybodies is easily derivable through the Stefan-Boltzmann law.

$$N_T = \frac{\epsilon \sigma T^4}{\pi} \tag{1}$$

where N_T = radiance at temperature T (W/M^2 /STER)

$\sigma = 5.67 \times 10^{-8}$ ($W/M^2/DEG^4$)

T = temperature (°K)

ϵ = emissivity

Assuming ϵ to be constant

$$\frac{dN_T}{dT} = \frac{4 \epsilon \sigma T^3}{\pi} \tag{2}$$

$$dN_T = \frac{4N_T dT}{T} \tag{3}$$

$$\left.\begin{aligned} dN_{300} &= 1.9\, \epsilon\, dT \\ dN_{260} &= 1.3\, \epsilon\, dT \\ dN_{200} &= 0.5\, \epsilon\, dT \end{aligned}\right\} \tag{4}$$

Since we will not be measuring total radiance, Planck's law should be used instead of the Stefan-Boltzmann law.

$$N_\lambda d\lambda = \frac{\epsilon_\lambda c_1 d\lambda}{\pi \lambda^5 \left(e^{\frac{c_2}{\lambda T}} - 1 \right)} \tag{5}$$

where $c_1 = 3.74 \times 10^8$ (for N_λ in $W/M^2/STER/\mu$)

$c_2 = 1.44 \times 10^4 \, \mu°K$

If we restrict T to values less than 320°K, then for the proposed spectral region we may approximate Eq. (5) by Wien's radiation law.

$$N_\lambda \, d\lambda = \frac{\epsilon_\lambda c_1}{\pi \lambda^5} \, e^{-\frac{c_2}{\lambda T}}, \quad \lambda T < 4{,}000 \, \mu °K \tag{6}$$

Assuming ϵ_λ to be independent of wavelength, temperature, scene material and equal to ϵ, differentiation of Eq. (6) with respect to temperature leads to

$$d\,(N_\lambda \, d\lambda) = \frac{c_2 N_\lambda \, d\lambda \, dT}{\lambda T^2}, \quad \lambda T < 4{,}000 \, \mu °K \tag{7}$$

The radiance $N_{\Delta\lambda}$ in the wavelength interval between λ_1 and λ_2 is

$$N_{\Delta\lambda} = \int_{\lambda_1}^{\lambda_2} N_\lambda \, d\lambda \tag{8}$$

$$\therefore \, dN_{\Delta\lambda} = \frac{c_2 \, dT}{T^2} \int_{\lambda_1}^{\lambda_2} \frac{N_\lambda \, d\lambda}{\lambda}, \quad \lambda T < 4{,}000 \, \mu °K \tag{9}$$

In the 10.5 to 12.5 micron region:

$$\left.\begin{aligned} dN_{\Delta\lambda}\,(300\,°K) &= 0.26 \, \epsilon \, dT \\ dN_{\Delta\lambda}\,(260\,°K) &= 0.18 \, \epsilon \, dT \\ dN_{\Delta\lambda}\,(200\,°K) &= 0.071 \, \epsilon \, dT \end{aligned}\right\} \tag{10}$$

B. Effect of An Emissivity Difference

For graybodies ϵ is independent of wavelength (by definition of graybody). However different graybodies may have different values of ϵ. As a fair approximation we may assume that in the 10.5 to 12.5 micron region, terrestrial features radiate as graybodies with small differences in emissivity. For this case Eq. (7) must be changed to

$$d(N_\lambda d\lambda) = \frac{c_2 N_\lambda d\lambda dT}{\lambda T^2} + N_\lambda d\lambda d\epsilon \tag{11}$$

$$d \int_{\lambda_1}^{\lambda_2} N_\lambda d\lambda = \frac{c_2 dT}{T^2} \int_{\lambda_1}^{\lambda_2} \frac{N_\lambda d\lambda}{\lambda} + d\epsilon \int_{\lambda_1}^{\lambda_2} N_\lambda d\lambda \tag{12}$$

$$\therefore dN_{\Delta\lambda} = \frac{c_2 dT}{T^2} \int_{\lambda_1}^{\lambda_2} \frac{N_\lambda d\lambda}{\lambda} + N_{\Delta\lambda} d\epsilon \tag{13}$$

In the 10.5 to 12.5 micron region:

$$\left.\begin{aligned} dN_{\Delta\lambda}\ (300\ ^\circ K) &= 0.26\ \epsilon\, dT + 18.6\ d\epsilon \\ dN_{\Delta\lambda}\ (260\ ^\circ K) &= 0.18\ \epsilon\, dT + 9.68\ d\epsilon \\ dN_{\Delta\lambda}\ (200\ ^\circ K) &= 0.071\ \epsilon\, dT + 2.24\ d\epsilon \end{aligned}\right\} \tag{14}$$

At 260°K a 4% emissivity difference is equivalent to a 2°C temperature difference. At 300°K a 3% change in ϵ is equivalent to a 2°C change in T.

C. S/N and NEΔT Calculations

The signal-to-noise ratio (S/N) of a radiometer can be defined as

$$S/N = \frac{\text{Signal Flux on Detector}}{\text{NEP of Dectector}}$$

$$= \frac{N_{\Delta\lambda} A_a \tau \Omega}{\text{NEP}}$$

where $N_{\Delta\lambda}$ = target radiance within spectral region $\Delta\lambda$

A_a = aperture area

τ = transmissivity of optics, including obscuration effects

Ω = solid angle I.F.O.V.

NEP = noise equivalent power

It will be assumed that the transmissivity of the medium between target and radiometer is unity and that a single detector cell is employed.

$$\text{Since} \quad \text{NEP} = \frac{\sqrt{A_d \Delta f}}{D^*_\lambda} \tag{16}$$

where A_d = detector area in cm^2

Δf = electronic bandwidth in Hz

D^*_λ = detector specific detectivity at wavelength λ in cm $Hz^{1/2}$ $watt^{-1}$

$$\therefore \text{S/N} = \frac{N_{\Delta\lambda} A_a \tau \Omega D^*_\lambda}{\sqrt{A_d \Delta f}} \tag{17}$$

For an I.F.O.V. that is square and small,

$$\Omega = \theta^2 \tag{18}$$

where θ = linear angular I.F.O.V. in radians.

If t is the frame time of a square picture with an angular width ϕ, then neglecting the return sweep time, the information bandwidth (assuming the low-frequency limit is 0) can be closely approximated by

$$\Delta f = \frac{1}{2} \frac{\left(\frac{\phi}{\theta}\right)^2}{t} \tag{19}$$

Substituting the above expressions for Ω and Δf into Eq. (17) we have

$$S/N = \frac{\sqrt{2}\, N_{\Delta\lambda}\, A_a\, \tau\, D^*_\lambda \sqrt{t}\, \theta^3}{\phi \sqrt{A_d}} \tag{20}$$

For a square detector cell,

$$\sqrt{A_d} = \ell \tag{21}$$

where ℓ= length of one side of square cell.

Also,

$$A_a = \frac{\pi D_a^2}{4} \tag{22}$$

where D_a = aperture diameter

$$\therefore S/N = \frac{\pi N_{\Delta\lambda}\, D_a^2\, \tau\, D^*_\lambda \sqrt{t}\, \theta^3}{2\sqrt{2}\, \phi \ell} \tag{23}$$

The above equation and also Eq. (20) seem to indicate that S/N is proportional to θ^3. This is misleading because, in a properly designed system, ℓ also depends on θ.

$$\ell = f\, \theta \tag{24}$$

where f = effective focal length.

Since the effective f-number (F) of the optical system is defined as

$$F = \frac{f}{D_a} \tag{25}$$

Eq. (23) can therefore be altered to reveal the dependence of S/N on θ.

$$S/N = \frac{\pi N_{\Delta\lambda} D_a \tau D^*_\lambda \sqrt{t}\, \theta^2}{2\sqrt{2}\, \phi F} \tag{26}$$

The above expression for S/N is rather optimistic because it does not include practical details such as amplifier noise and the effect of radiation chopping on signal amplitude. Also, it is important to modify the value of D^*_λ given by the detector manufacturer to reflect differences in the radiometer operating conditions from those used in the detectivity measurement. If we let α be the adjustment factor that transforms Eq. (26) into a realistic expression for S/N, then

$$S/N = \frac{1.11\, N_{\Delta\lambda} D_a \tau D^*_\lambda \sqrt{t}\, \theta^2}{\alpha \phi F} \tag{27}$$

When S/N = 1, $N_{\Delta\lambda}$ is called the noise equivalent radiance (NER). The S/N for a target at temperature T can therefore be expressed as

$$S/N = \frac{N_{\Delta\lambda}(T)}{NER} \tag{28}$$

where

$$NER = \frac{0.90\, \alpha \phi F}{D_a \tau D^*_\lambda \sqrt{t}\, \theta^2} \tag{29}$$

Eq. (27) is the expression for S/N for a single resolution element of radiance $N_{\Delta\lambda}$. When the target radiance differs from the background by an amount of $dN_{\Delta\lambda}$ the ability to discriminate between the two is measured by the S/N associated with $dN_{\Delta\lambda}$ rather than $N_{\Delta\lambda}$. Now

$$dN_{\Delta\lambda} = \left(\frac{dN_{\Delta\lambda}}{dT}\right)_T dT \tag{30}$$

where dT = temperature differential between target and background

$\left(\frac{dN_{\Delta\lambda}}{dT}\right)_T$ = rate of change of $N_{\Delta\lambda}$ with temperature at background temperature T.

As an approximation we shall assume that

$$\Delta N_{\Delta\lambda} = \left(\frac{dN_{\Delta\lambda}}{dT}\right)_T \Delta T \tag{31}$$

where $\Delta T \ll T$. Replacing $N_{\Delta\lambda}$ in Eq. (27) by $\Delta N_{\Delta\lambda}$ and using Eq. (31) we have

$$(S/N)_{\Delta T,T} = \frac{1.11 \left(\frac{dN_{\Delta\lambda}}{dT}\right)_T \Delta T \, D_a \, \tau \, D^*_\lambda \sqrt{t} \, \theta^2}{\alpha \phi F} \tag{32}$$

Plots of $N_{\Delta\lambda}$ and $(dN_{\Delta\lambda}/dT)_T$ vs T for a blackbody between 10.5 and 12.5 microns are shown in Fig. 2.

By definition, the noise equivalent temperature difference (NEΔT) is the value of ΔT for which $(S/N)_{\Delta T} = 1$.

$$\therefore (NE\Delta T)_T = \frac{0.90 \, \alpha \phi F}{\left(\frac{dN_{\Delta\lambda}}{dT}\right)_T D_a \, \tau \, D^*_\lambda \sqrt{t} \, \theta^2} \tag{33}$$

Comparing Eqs. (29) and (33) we see that

$$NER = (NE\Delta T)_T \left(\frac{dN_{\Delta\lambda}}{dT}\right)_T \tag{34}$$

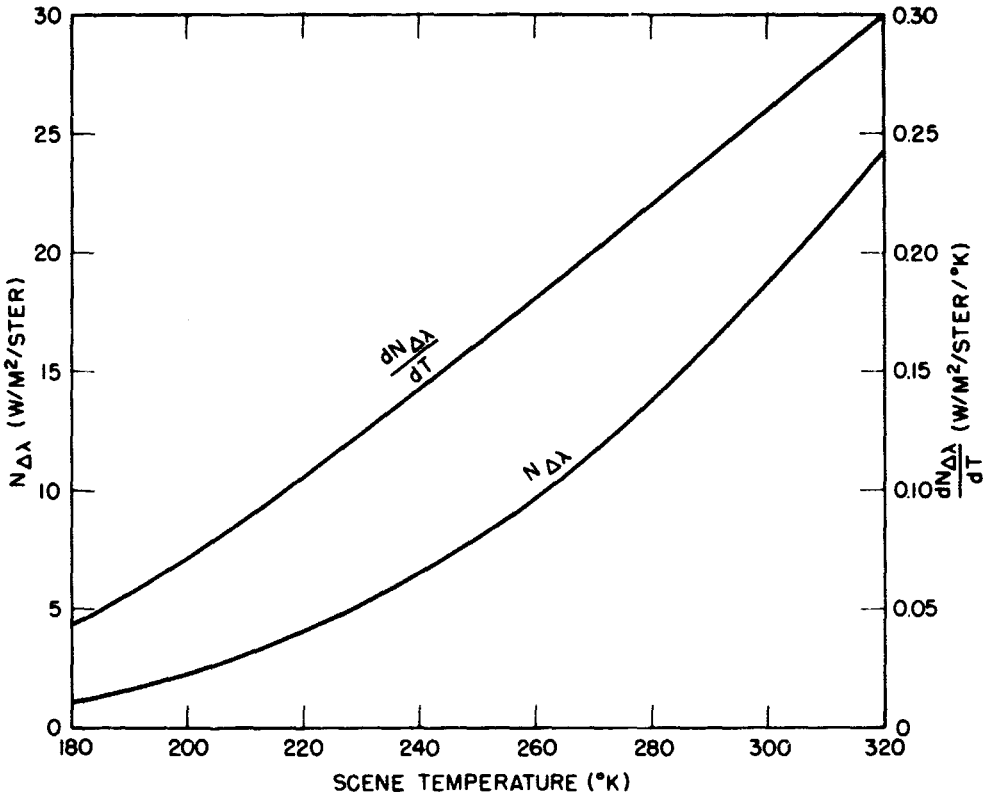

Figure 2–$N_{\Delta\lambda}$ and $\frac{dN_{\Delta\lambda}}{dT}$ VS Temperature For The 10.5-12.5 Micron Region

It is of interest to note that NER does not depend on scene temperature. It is strictly an instrument function. If we require that the NEΔT for a scene temperature of 200°K be no greater than 3°C then the radiometer must have an NER less than or equal to 0.21 W/M^2/STER. As we shall see below this can likely be attained for an I.F.O.V. of 0.3 mrad but is very difficult to achieve for 0.15 mrad. A plot of NEΔT and S/N as a function of scene temperature, assuming an NER value of 0.21 W/M^2/STER is shown in Fig. 3.

The noise equivalent temperature (NET) can be defined as the temperature for which $N_{\Delta\lambda}$ = NER. The relationship between NET and NER for the 10.5–12.5 micron region is shown in Fig. 4. For the proposed NER value of 0.21 W/M^2/STER the NET is 145°K.

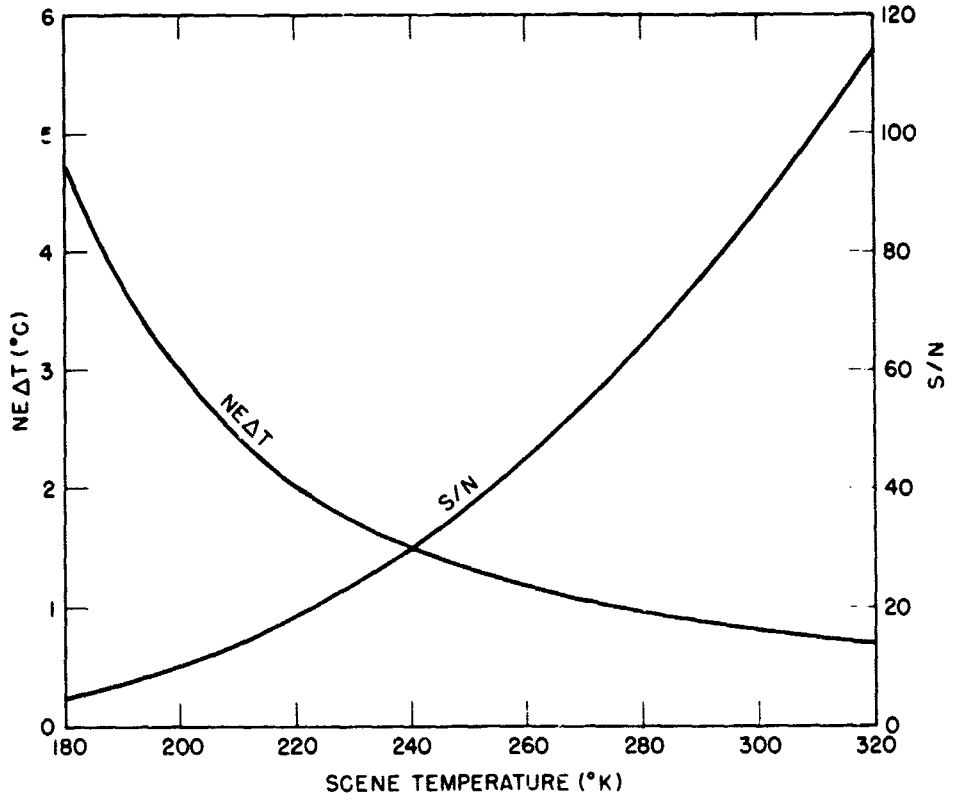

Figure 3–NEΔT and S/N VS Temperature for NER = 0.21 W/M^2/STER

For ϕ = .314 rad (18°), F = 1.5, τ = .4, $D^* = 1.5 \times 10^{10}$, t = 1200 sec and D_a = 20 cm (8 inches) the value of NER from Eq. (29) becomes

$$\left.\begin{aligned} \text{NER} &= \frac{10^{-13}\,\alpha}{\theta^2}\ \text{w/cm}^2\text{/ster} \\ &= \frac{10^{-9}\,\alpha}{\theta^2}\ \text{w/M}^2\text{/ster} \end{aligned}\right\} \qquad (35)$$

Assuming that radiation chopping will be employed,

$$\alpha = 6.1,\ \theta = 0.15\ \text{mrad}$$

$$= 5.7,\ \theta = 0.3\ \text{mrad}$$

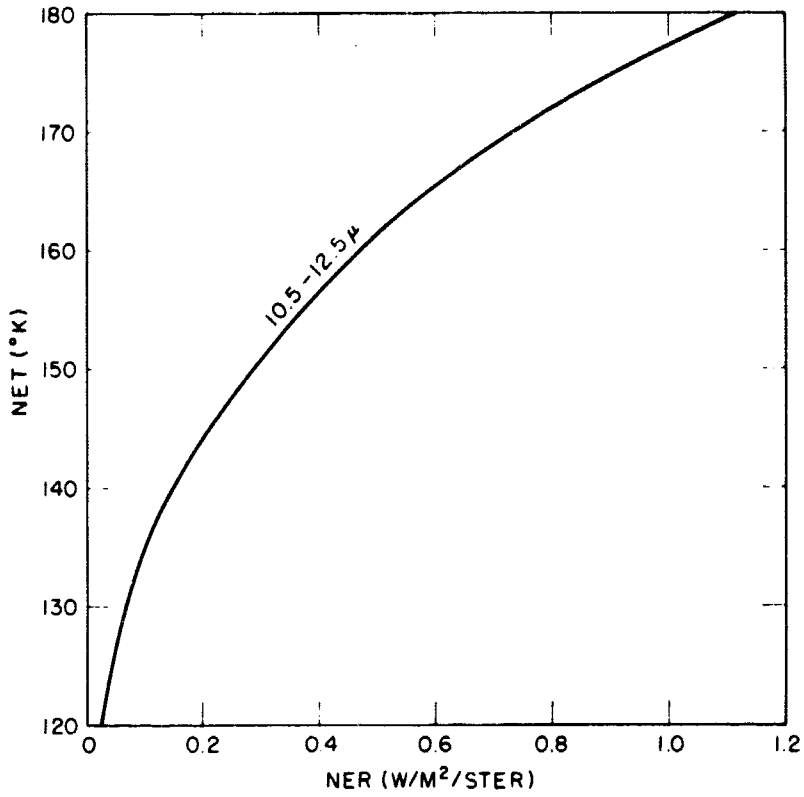

Figure 4–NER VS NET for the 10.5-12.5 Micron Region

The calculations involved in determining α are given in the next section.

$$\therefore \text{NER} = 0.27\ \text{W/M}^2\text{/STER},\ \theta = 0.15\ \text{mrad}$$

$$= 0.063\ \text{W/M}^2\text{/STER},\ \theta = 0.3\ \text{mrad}$$

Not only is there a sensitivity problem for $\theta = 0.15$ mrad but, due to diffraction, the effective I.F.O.V. is significantly larger than 0.15 mrad (see section IV F). Also, the detector size required, 0.0018 inch (45 microns) on a side, puts an added burden on the detector manufacturer. The proposed 0.3 mrad I.F.O.V. design considerably improves the situation with a relatively small sacrifice in effective resolution. With the proposed system a degradation of a factor of 3 in S/N can be tolerated (assuming the previously mentioned NEΔT requirement of 3°C at 200°K). If the system should not be degraded at all, then for $\theta = 0.3$ mrad,

$$(NE\Delta T)_{200} = 0.90\ ^\circ C$$

$$(NE\Delta T)_{300} = 0.24\ ^\circ C$$

D. The Adjustment Factor α

There are several quantities which must be estimated in order to arrive at a realistic value of α for a particular radiometer design. For example, the value of D^* associated with a detector is valid for a certain set of conditions. If the detector is to be used under different conditions then a factor must be included to reflect this. In general the value of α will be the product of the following factors:

α_1 – detector operating conditions

α_2 – effective noise bandwidth

α_3 – chopping

α_4 – electronic filter response

α_5 – system noise

α_6 – diffraction

The magnitude and product of the factors are given in Table 2.

Table 2. Estimates of the Adjustment Factors for the Proposed Radiometer for two Values of the Geometric Instantaneous Field of View (G.I.F.O.V.)

Factor	G.I.F.O.V. = 0.15 mrad		G.I.F.O.V. = 0.3 mrad	
	Electronic Chopping	Radiation Chopping	Electronic Chopping	Radiation Chopping
α_1	1.15	1.0	2	1.1
α_2	2.8	1.41	2.5	1.41
α_3	1.57	1.57	1.57	1.57
α_4	1.05	1.05	1.15	1.15
α_5	1.7	1.7	1.7	1.7
α_6	1.54	1.54	1.20	1.20
Product	13.9	6.09	18.4	5.71

The details in estimating the factors are given below.

1. Detector operating conditions (α_1)

It is common practice to give the value of D^* for the following conditions:

(a) optimum detector bias voltage
(b) optimum modulation or chopping frequency
(c) optimum operating temperature
(d) infinite load resistance
(e) at peak wavelength

a. For thermistor bolometers optimum bias is seldom used because of possible damage to the detector. For photoconductors requiring a high bias voltage, the optimum is sometimes not used because it isn't convenient. For our photoconductor case the optimum voltage is very low and therefore is not a problem.

b. If radiation chopping is used the detector can be made to operate near the optimum modulation frequency. If it is not employed there is considerable degradation due to low frequency detector noise. Most of this goes into increasing the effective noise bandwidth which will be calculated in the next section 2. However the value of D^*_λ that must be used is that at the upper information frequency limit (in general it must be at the frequency within the information bandwidth for which D^*_λ is a maximum). For θ = 0.3 mrad the upper information frequency is approximately 450 Hz. For our detector the value of D^*_λ at this frequency is about 1/2 that at optimum frequency. The degradation factor is therefore 2. For θ = 0.15 mrad the degradation factor is 1.15. This is in addition to the degradation factor computed for the effective noise bandwidth.

Although it is possible to optimize the chopping frequency, this may not be convenient because it can be as high as 10,000 Hz or more. Not to be overly optimistic, we shall assume that the chop frequency used introduces a degradation factor of 1.1 for θ = 0.3 mrad (and 1.0 for θ = 0.15 mrad).

c. If a sublimation cooler is employed there should be no problem in operating the detector within the optimum temperature range. If a radiation cooler is used, this may be difficult to accomplish. However, we shall assume that the radiometer will have a sublimation cooler and therefore there will be no degradation associated with the detector operating temperature.

d. If the load resistance is equal to that of the detector (as is usual with bolometer circuits) then D^* must be reduced by a factor of $\sqrt{2}$. This is because responsivity drops by a factor of 2 (compared to open circuit) while the circuit noise drops by only $\sqrt{2}$. With a photodetector there is usually no compelling reason to use a matched load. For practical reasons it is not feasible to supply the detector with optimum bias current through an infinite load resistor. However, the detector that will be used has little resistance and requires only a small bias current so that the infinite load condition can be closely approximated.

e. The appropriate detector has its peak spectral response within the 10.5-12.5 micron region. The D^*_λ value of 1.5×10^{10} that was assumed in the calculations was intended to represent the average value in this spectral region. This is not overly optimistic for two reasons, (1) D^*_λ values higher than 1.5×10^{10} have been measured within this region and (2) additional gain is possible with a cooled aperture since the best photodetectors in this region are background noise limited.

In summary, the adjustment factor associated with detector operating conditions is

θ = 0.15 mrad

α_1 = 1.15 (electronic chopping)
= 1.0 (radiation chopping)

θ = 0.3 mrad

α_1 = 2 (electronic chopping)
= 1.1 (radiation chopping)

2. Effective noise bandwidth (α_2)

a. No radiation chopping

For ϕ = .314 radians (18°), t = 1200 sec (20 minutes) and θ = 0.3 mrad the information bandwidth according to Eq. (19) is 456 Hz. If space is used as a zero signal reference and the baseline is dc restored every 1.2 seconds the effective lower cutoff frequency is 0.85 Hz. Since the detector suffers from 1/f noise throughout the entire information spectrum the effective noise bandwidth Δf_N, assuming no radiation chopping, can be approximated by

$$\Delta f_N = f_2 \ln \frac{f_2}{f_1} \tag{36}$$

where f_1 and f_2 are the lower and upper cutoff frequencies, respectively. For $f_1 = 0.85$ Hz and $f_2 = 456$

$$\Delta f_N = (456)\ (6.29) = 2{,}866 \text{ Hz}$$

Thus the noise bandwidth is about 6.3 times as high as the information bandwidth. Since S/N is inversely proportional to $\sqrt{\Delta f}$, the noise bandwidth degradation factor is 2.5. For $\theta = 0.15$ mrad, the factor is 2.8. Therefore, if radiation chopping is not employed

$$\alpha_2 = 2.8,\ \theta = 0.15 \text{ mrad}$$

$$= 2.5,\ \theta = 0.3 \text{ mrad}$$

b. Radiation chopping

When radiation chopping is used the electronic bandwidth must be twice the information bandwidth in order to obtain the information in the side bands on both sides of the chop frequency. Thus the degradation factor is

$$\alpha_2 = 1.41$$

3. Chopping (α_3)

In a typical system that employs radiation modulation, a reference blackbody is brought into the detector's F.O.V. every half cycle and the signal, after amplification, is synchronously demodulated. If the chop frequency is high enough the detector low frequency (1/f) noise is eliminated. Radiation modulation also allows the use of an a.c. amplifier (rather than the more troublesome d.c. amplifier). An electronic chopper (signal modulation after preamplification) also permits the use of a.c. amplifiers but does not suppress the low frequency detector noise. For either type of chopper that generates a square wave signal the amplitude of the fundamental modulation frequency is $2/\pi$ that of the unmodulated signal amplitude. For the radiation modulation case a square wave will be created only if the chopper aperture is much larger than the image that is chopped. If the aperture of the chopper is, say, twice as large as the modulated image then the resulting trapezoidal wave signal will cause a degradation factor of 1.9, instead of 1.57 for the square wave case. We shall assume that the chopper aperture is much larger than the image. Therefore, for both electronic and radiation chopping,

$$\alpha_3 = 1.57$$

4. Electronic filter response (α_4)

Ideally, if a target one resolution element wide is scanned, the detector signal output shape is triangular (if a point source were scanned the signal shape would be rectangular with a base width half that of the triangular wave). In order to process all the information in the signal a very large bandwidth is required. However this is not desirable since an unduly large amount of noise would also be added to the system. An optimum upper bandwidth limit for such a pulse is approximately $1/2\ t_d$, where t_d is the dwell time for a point source. For this bandwidth limit the actual signal level is 78% of that using infinite bandwidth. For this case (triangular pulse) the degradation factor is therefore 1.28. However, because of diffraction, the signal will be bell shaped with an increased base width, resulting in a smaller degradation factor. Since the diffraction effect is greater for smaller θ values, the base width is larger for $\theta = 0.15$ mrad than it is for $\theta = 0.3$ mrad. Therefore α_4 is smaller for the 0.15 mrad I.F.O.V. case. We estimate the filter response factor to be

$$\alpha_4 = 1.05,\ \theta = 0.15 \text{ mrad}$$

$$= 1.15,\ \theta = 0.3 \text{ mrad}$$

5. System noise (α_5)

In addition to increasing the signal level an amplifier also introduces additional noise into the system. Present day transistor amplifiers are very good and there should be no trouble in designing a preamplifier with a 3db noise figure or a degradation factor of 1.4. Unfortunately, other sources of noise generally appear after the radiometer is built and placed on a fully operating spacecraft. This extra noise is rarely, if ever, completely eliminated. Even in the less hostile environment of a laboratory it is unlikely that the radiometer by itself will be entirely free of nonessential noise. We estimate the circuit noise factor as

$$\alpha_5 = 1.7$$

This does not include the degradation in data transmission and ground station processing which we cannot estimate at the present time, but it should be small.

6. Diffraction (α_6)

Because of diffraction not all of the energy which comes from the target (defined by the geometric instantaneous field of view) falls on the detector. Table 3 shows the relative amount of diffracted radiation which originates from the target and that is contained within image areas of 1.0, 1.25 and 1.50 times the G.I.F.O.V. (geometric instantaneous field of view) for a typical folded optical system. For $\theta = 0.15$ mrad only 52% of the radiation within the G.I.F.O.V. strikes the detector (assumed to be circular for ease in the diffraction calculations). However, for a uniform extended source, the lost energy is regained by diffracted energy which comes from outside the G.I.F.O.V. This has the effect of degrading the spatial resolution of the radiometer and will be discussed more fully in section IV F. From a strict point of view, the degradation factor α_6 should be based on the values given in Table 3 under the 1.0 G.I.F.O.V. column. Actually this is too severe since a significant additional amount of energy comes from the immediate neighborhood of the target. We shall arbitrarily select the 1.25 G.I.F.O.V. column for estimating α_6. This is not overly conservative, especially when it is realized that the optical relay will further disperse the energy. Therefore

$$\alpha_6 = 1.54, \ \theta = 0.15 \text{ mrad}$$

$$= 1.20, \ \theta = 0.3 \text{ mrad}$$

Table 3. Relative amount of diffracted 12 micron radiation falling in the image plane for a perfect folded telescope with an 8-inch aperture. The ratio of the central obscuration to aperture diameters is 0.4.

G.I.F.O.V. (mrad)	Diffracted Energy Within		
	1.0 G.I.F.O.V.	1.25 G.I.F.O.V.	1.50 G.I.F.O.V.
0.15	.52	.65	.74
0.30	.70	.83	.88
0.45	.78	.89	.93

E. The 10.5-12.5 Micron Region

Spectral regions in which the atmosphere transmits radiation with comparatively little attenuation are called windows. The 8-13 micron atmospheric window covers a spectral region that contains most of the surface emission that reaches space. The window is bounded on the lower wavelength side by water

vapor absorption and on the upper side by carbon dioxide. An intense ozone band is centered at 9.6 microns. For a zenith path from the earth's surface to space for a representative atmosphere the width of the ozone band is about 1.2 microns (at the 50% points). Ozone concentration can vary by a factor of 2. Carbon dioxide absorption is negligible below 12.5 microns, but water vapor absorption is noticeable throughout the window. The cleanest portion of the window lies between 10.5 and 11 microns. Although widening the bandwidth increases the radiation received at the detector it also increases the temperature error and makes surface temperature discrimination more difficult. A good compromise seems to be the region between 10.5 and 12.5 microns. Opening the bandwidth still further to, say, 8.5-12.5 microns would result in an increase in both surface and ozone radiation in roughly equal amounts.

F. Diffraction Effects

For a circular, clear aperture, paraboloidal mirror and a point source on axis at infinity, the angular radius (ρ_A) of the Airy disk (central bright area of the diffraction pattern) is

$$\rho_A = \frac{1.22\lambda}{D_a} \tag{37}$$

where λ = radiation wavelength and D_a = aperture diameter. This formula is also the expression for the Rayleigh criterion for the resolution of two point sources of equal intensity. The Airy disk contains approximately 84% of the total diffracted energy of wavelength λ. The remainder is distributed in circular concentric rings as shown in Table 4.

Table 4. Energy and size of diffraction rings for a circular clear aperture paraboloidal mirror. One Airy unit is equal to $1.22\lambda/D_a$.

Ring (Bright)	Proportion of Total Diffracted Energy in Each Ring	Outer Ring Angular Radius in Airy Units
Airy Disk	.838	1
Second	.071	1.82
Third	.028	2.66
Fourth	.015	3.48
Fifth	.01	4.26

The proposed telescope does not have a clear aperture but contains a secondary mirror which acts as a central obscuration. Also, the target is extended and not two point sources. These factors have a marked effect on the diffraction pattern and therefore on spatial resolution. For extended sources the image can be thought of as the sum of the diffraction patterns of all the "points" making up the source (the location of the diffraction center of each "point" is given by geometrical optics). Table 5 lists the values of the image angular diameters containing various fractions of the diffracted energy from the corresponding source angular diameter. The telescope aperture is assumed to have a diameter of 8 inches and λ = 12.3 microns. The source angular diameter is equivalent to the G.I.F.O.V. of the proposed radiometer. The central obscuration diameter is assumed to be 0.4 D_a.

Table 5. Image angular diameter as a function of source diameter at 50%, 75%, 84%, 90% and 95% energy points. The telescope aperture diameter is 8 inches, the central obscuration diameter is 0.4 D_a and λ = 12.3 microns.

Source Angular Diameter (mrad)	Image Angular Diameter (mrad)				
	50%	75%	84%	90%	95%
.15	.15	.23	.30	.41	.83
.20	.18	.26	.33	.43	.84
.25	.21	.29	.36	.45	.85
.30	.24	.32	.39	.48	.86
.35	.27	.36	.42	.51	.88
.40	.31	.40	.46	.55	.90
.45	.34	.44	.50	.59	.92

In situations where the S/N is sufficiently high it is common practice by many scanning radiometer designers to assume that the limiting angular resolution of the optical system is the angular diameter of the Airy disk as defined for an unobstructed paraboloidal mirror and a distant point source on axis. For a perfect telescope with an aperture diameter of 8 inches and λ = 12.3 microns the Airy disk diameter is 0.15 mrad. If the telescope has a central obscuration with a diameter equal to 0.4 D_a and the G.I.F.O.V. is also 0.15 mrad only 52% of the radiation coming from within the G.I.F.O.V. falls on the detector (assumed circular for simplicity in analysis). The remainder of the diffracted energy is spread out over the image plane. If the background is also at the same temperature then 48% of the radiation falling on the detector comes from outside the G.I.F.O.V. If the background is at a higher temperature (as would be the case for a small cloud cell surrounded by warmer land or sea below) the "outside

energy" could easily be greater than the "inside energy." It is obvious that, under these conditions, a temperature measurement of a cloud cell the size of an Airy disk will not be at all accurate. The situation is different for much larger clouds. Here the average temperature of the cloud top surface can be measured much more accurately since the "outside energy" will be from the cloud top also (except at the cloud edges). However, cloud detail of Airy disk size will not be measured very well – height variations up to a km along the cloud surface will not be detected at all, while breaks in clouds will appear bigger and cooler than they actually are. If the G.I.F.O.V. is increased from 0.15 mrad to 0.3 mrad the effective spatial resolution will not be degraded by a proportionate amount. If we use the 75% energy points as a criterion then the effective resolution is poorer by a factor of 1.4. If the 90% points are used the resolution is degraded by only 17%. By analogy to the Airy disk energy (point source and clear aperture) it seems reasonable to take the 84% points as the criterion for the effective spatial resolution. This is not overly conservative because the system resolution is actually worse than indicated in Table 5. Additional degradation is caused by the optical relay and the spider (secondary mirror supporting members). A spider of four legs produces a point source diffraction pattern of 8 lines, 4 large ones in the shape of a plus (+) sign and 4 smaller ones at an angle of 45° with the larger ones. It is the spider that is responsible for the "radiating" lines that sometimes appear in the image of a bright star taken with a diffraction limited folded telescope.

Because of diffraction effects therefore, the effective spatial resolution of the proposed radiometer is estimated as 0.4 mrad. This corresponds to an effective subsatellite ground resolution of about 8 n.mi.

It may be possible to improve the resolution of the telescope by a technique called apodization, which is used to suppress the secondary maxima of the diffraction pattern. For circular apertures, apodization is accomplished by means of a variable transmission aperture stop that is clear at the center and with continuously increasing attenuation in the radial direction. This has the effect of eliminating the main contribution to the energy in the higher order diffraction pattern – that due to the sharp discontinuity at the rim of the entrance aperture. Although not a routinely practiced technique, apodization has been used to resolve some double stars with telescopes that normally did not have this resolution capability. However, for our application there are other factors that should be considered. First, the diameter of the Airy disk is increased by apodization (from 20% to 40%). Second, the total transmission of the telescope is reduced (by a factor of 2 or more). Third, apodization is not as effective on folded telescopes as on those with clear apertures. Fourth, apodization works better for point sources than for extended objects. Taking these items into account, it is not clear that apodization is worthwhile for the proposed experiment.

V. SUMMARY

At geosynchronous altitude a radiometer containing an 8-inch diameter telescope and a cooled detector sensitive to the 10.5 to 12.5 micron region can continuously observe cloud cover and make accurate surface temperature measurements with an effective subsatellite ground resolution of approximately 8 nautical miles. An experiment using such a radiometer is proposed for ATS F&G. Since cloud top altitudes are obtainable through the temperature measurements, wind speeds at cloud top heights can be inferred from the radiometric data. Land and sea surface temperatures in cloud free regions will also be measured as well as temperature variations such as those due to the Gulf Stream. Because the radiometer operates in the 10.5 to 12.5 micron atmospheric window "full earth" pictures containing all the valuable temperature information will be taken on every frame both night and day.

It appears that the poor location space available on the ATS spacecraft for this experiment does not permit use to be made of a radiative cooler. About 60% of the estimated total weight of 110 pounds is due to the solid cryogen refrigerator necessary to cool the detector to 77°K.

The analysis shows that the major limitation to spatial resolution is due to diffraction in the optical system. For this reason it is possible to design the radiometer so that it has very good absolute and relative temperature accuracy with little sacrifice in effective spatial resolution. Because the detector suffers from low frequency noise it is recommended that radiation chopping be employed. If this is not done the S/N will be degraded by a factor of 3 and the temperature accuracy will be reduced.